Journal of
Marine Science and Engineering

MDPI

Article

Experimental and Estimation Studies of Resilient Modulus of Marine Coral Sand under Cyclic Loading

Shao-Heng He [1], Qiong-Fang Zhang [2,*], Zhi Ding [3,*], Tang-Dai Xia [1] and Xiao-Lu Gan [1]

1 Research Center of Coastal and Urban Geotechnical Engineering, Zhejiang University, Hangzhou 310058, China; heshaoheng@zju.edu.cn (S.-H.H.); xtd@zju.edu.cn (T.-D.X.); xlgan@zju.edu.cn (X.-L.G.)
2 Power China Huadong Engineering Corporation, Hangzhou 310014, China
3 Department of Civil Engineering, Zhejiang University City College, Hangzhou 310015, China
* Correspondence: zhang_qf2@ecidi.com (Q.-F.Z.); dingz@zucc.edu.cn (Z.D.)

Received: 17 March 2020; Accepted: 14 April 2020; Published: 16 April 2020

check for updates

Abstract: Coral sand is an important filler resource that can solve the shortage of terrestrial fillers in coastal areas. Recently, the foundations of many infrastructures in the South China Sea have been built with coral sand as fillers, which have been subjected to wave and traffic cyclic loads. Resilient modulus (M_r) is an important design parameter in marine engineering, but there are few studies on the resilient modulus response of coral sand under cyclic loading. A series of drained cyclic triaxial tests were carried out to investigate the effects of the initial mean effective stress (p_0) and cyclic stress ratio (ζ) on the resilient modulus response of the coral sand from the South China Sea. The change of fractal dimension (α_c) can reflect the rule of particle breakage evolution. The α_c of coral sand shows a tendency of almost maintaining stable and then increasing rapidly with the increase of mean effective stress p_0 under each cyclic stress ratio ζ. There is a threshold of p_0, when the p_0 exceeds this threshold, α_c will increase significantly with the increase of p_0. The increase of p_0 has a beneficial effect on the improvement of the M_r, while the increase of ζ has both beneficial and detrimental effects on the improvement of the M_r. A new prediction model of the M_r considering particle breakage was established, which can better predict the M_r of coral sand in the whole stress interval. The research results can provide guidance for the design of marine transportation infrastructures, which can promote the development of marine transportation industry and energy utilization.

Keywords: coral sand; resilient modulus; particle breakage; fractal dimension; prediction model

1. Introduction

Coral sand is widely distributed in the equatorial and tropical marine areas, which is the foundation soil type encountered in many marine engineering construction [1–3]. Coral sand is formed by the deposition of marine biological debris, and its main component is calcium carbonate. The mechanical properties of coral sand are totally different from that of terrigenous quartz sand [4–7]. For example, its particles are irregular in shape and easy to break under external load. Recently, many reef island infrastructures for land reclamation in the South China Sea have used coral sand as foundation filling materials. Coral sand has now been used as foundation filling materials in the construction of airport runways, flexible road pavements, building foundations, and other infrastructures. In the complex marine engineering environment, the hydraulic filling coral sand foundation will be subject to tens of thousands of low frequency traffic and wave cyclic loads for a long time. Resilient modulus is an important parameter for the evaluation and design of bearing capacity, settlement deformation, and service performance of foundation soil under cyclic loading [8–10]. Therefore, it is of great significance to study the response and prediction model of resilient modulus of coral sand under cyclic loading.

Numerous experimental studies (mainly based on cyclic triaxial tests) have been carried out on resilient behavior of unbound granular materials, which is usually represented by the resilient modulus M_r [10–12]. The studies, based on the resilient characteristics of unbound granular materials, focused on the terrigenous materials, such as ballast and quartz sand. Hicks [13] stated that frequency has a negligible effect on the elastic behavior of granular materials. Lackenby et al. [14] emphasized that for railway ballast, M_r increases with the increase of load cycles N, mean effective stress p', and cyclic deviatoric stress q_{ampl}. Indraratna et al. [15] examined the effect of p' and f on M_r. It was found that M_r increases with the increase of p' and f, which was due to the increase of packing density. Donohue et al. [16] reported that some coarse-grained soil used as subgrade fillers will undergo particle degradation under cyclic loading. Particle degradation includes particle breakage and fine-grain intrusion mainly caused by particle breakage [17,18]. Particle breakage can lead to adverse effects, such as the reduction in shear strength, interlocking, and stiffness of soil aggregates [19,20]. Different empirical models have been reported for the estimation of resilient modulus M_r of unbound granular materials under cyclic loading [21,22]. However, Chen et al. [21] found that for some coarse-grained soils degraded under cyclic loading, a good fitting curve based on the full stress interval will obviously underestimate the resilient modulus of the low stress interval. This is a challenging problem, which deserves more research to investigate the M_r's prediction model of coral sand under the whole stress interval. Due to its unique mineral composition and mechanical properties, coral sand will undergo more serious particle degradation (i.e. particle breakage) under cyclic loading than terrigenous materials. Current experimental studies on coral sands focused on the static shear behavior [1,3,6], influencing factors for particle breakage [2], and small strain dynamic characteristics [4,23]. At present, the research on resilient behavior of coral sand under cyclic loading is relatively lacking. There is still no clear understanding of the resilient modulus of coral sand in engineering.

In this paper, a series of drained cyclic triaxial tests were carried out on the coral sand of the South China Sea to investigate the resilient modulus M_r response. The evolution of particle breakage of coral sand was studied by analyzing the variation of fractal dimension α_c during cyclic loading. The effects of the initial mean effective stress p_0 and cyclic stress ratio ζ on the M_r were examined. The influence of particle breakage on the prediction model of M_r was deeply analyzed. Finally, a new resilient modulus prediction model for coral sand considering particle breakage was established. This study can help deepen the understanding of the resilient behavior of coral sand, which is beneficial to the design and safety assessment of marine transportation infrastructures.

2. Materials and Methods

2.1. Test Materials and Sample Preparation

The coral sand samples were taken from an offshore reef in the South China Sea, which were all unbound particles (as shown in Figure 1a). Figure 1b shows the microparticle shape of coral sand obtained by scanning electron microscopy (SEM). It can be seen from Figure 1b that the grain shape of the coral sand sample is irregular and retains a large amount of the internal pores of the original marine biological debris. Figure 2 shows the particle size distribution curve of the coral sand sample. Table 1 presents the basic physical and mechanical parameters of test sand samples.

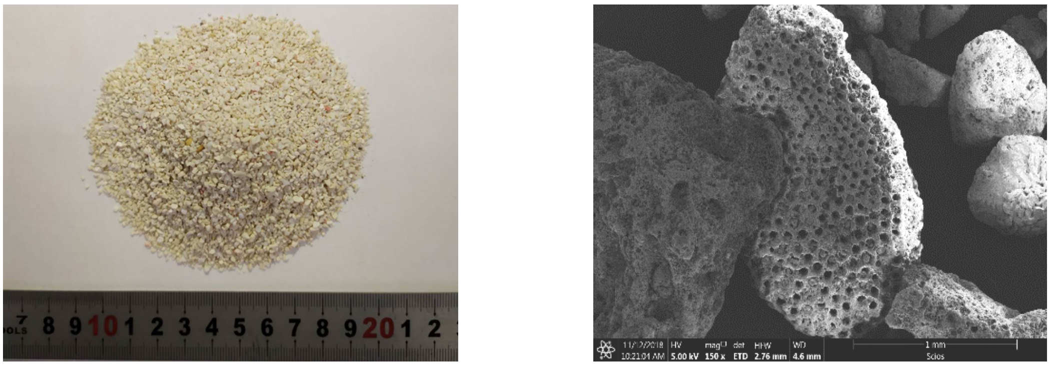

(a) (b)

Figure 1. Typical sample of the coral sand: (**a**) coral sand sample; (**b**) microparticle shape of coral sand.

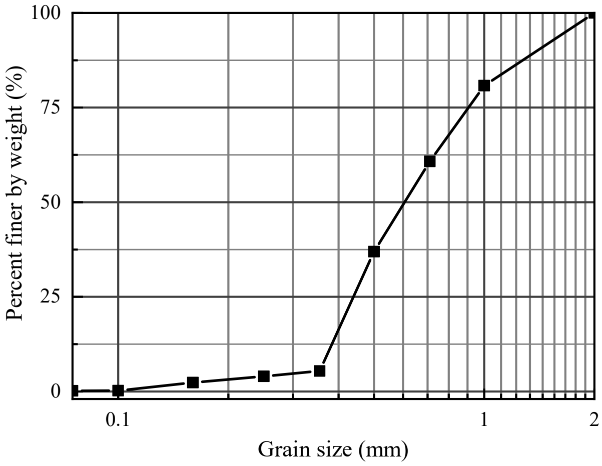

Figure 2. Particle size distribution curve of coral sand samples.

The cyclic triaxial sample in this study was a standard cylinder sample with a height of 100 mm and a diameter of 50 mm. Since the prediction model of resilient modulus is mainly used in the design of compact foundations such as road bases, previous studies on the resilient behavior of soils have used dense samples [11]. Due to the strict requirements of relative density D_r of the road bases, wharfs and other marine engineering infrastructures, the foundation of hydraulic filling coral sand is very dense. Therefore, in order to meet the actual engineering characteristics, the relative density D_r of the coral sand samples in this study were selected as 80%. The air pluviation method [23] was applied to prepare cylindrical samples of the coral sand. The method of light hammering was used to obtain the designed relative density of sand samples. The samples were remolded for $D_r < 80\%$, depending on the initial consolidation stress, to acquire the target D_r (i.e., 80%) after consolidation. After the preparation of the sample, carbon dioxide (CO_2) was used to pass through the sample, and then the sample was saturated with 200 kPa back pressure under the effective confining pressure of 20 kPa. After checking that the B-value of the sample exceeded 0.95, the saturation process of the sample ended. Through K_0 (static earth pressure coefficient) consolidation module of triaxial apparatus [24,25], the K_0-value of coral sand sample was set at 0.4. After the sample was saturated, the sample was consolidated under anisotropic condition. During consolidation, the σ_3/σ_1-value (σ_1 and σ_3 are the major and minor principal stress, respectively) was fixed to the K_0-value to simulate K_0 consolidation.

Table 1. Basic physical and mechanical parameters of test sand samples.

Property	Coral Sand
Specific gravity (G_s)	2.75
Maximum void ratio (e_{max})	1.107
Minimum void ratio (e_{min})	0.971
Coefficient of uniformity (C_u)	1.793
Coefficient of curvature (C_c)	0.781
Relative density of samples (D_r)	80%

2.2. Test Methods

The cyclic triaxial apparatus [26] developed by GDS company (GDS Instruments Ltd., UK) was used in this study, which includes a loading system, a back pressure volume controller, a confining pressure volume controller, a pore pressure sensor, displacement and force sensors (as shown in Figure 3). The pressure chamber base is connected with various sensors and pressure volume controllers, including back pressure, confining pressure, pore pressure, etc. The axial force is measured at a load cell being located directly below the bottom end plate of the sample, i.e., inside the cell chamber. The axial deformation is obtained from a displacement transducer attached to the load piston (not shown in Figure 3).

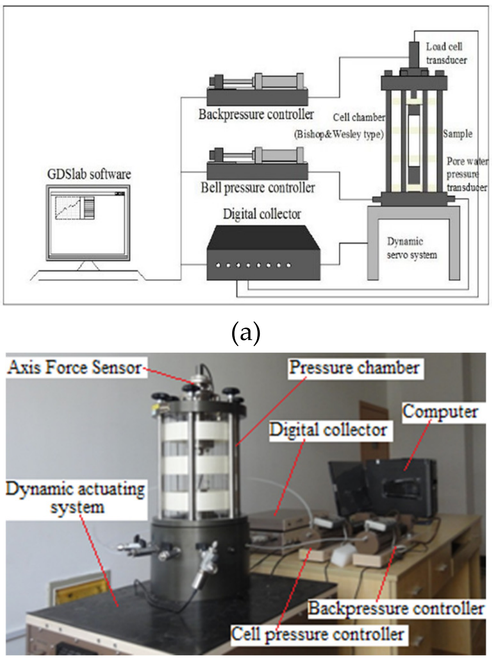

(a) (b)

Figure 3. Cyclic triaxial apparatus used in this study: (**a**) schematic diagram of cyclic triaxial apparatus system; (**b**) cyclic triaxial apparatus.

Chen et al. suggested using 1 Hz as the frequency of the resilient response tests for granular soils [21]. With reference to previous studies, the effect of frequency f on the resilient behavior of coarse-grained soil can be ignored [14]. In order to ensure the stability of data collection, the frequency f of cyclic loading was selected as 0.5 Hz in this study. In order to study the long-term resilient response of coral sand, the number of cycles N was selected to be 20,000. Referring to the experimental studies of coarse-grained soil under traffic cyclic loading by other scholars, the cyclic loading type of this study used half-sine loading [27–29]. Drained cyclic triaxial tests were performed on coral sand samples at p_0 = 40, 70, 100, 200, 300, 400 kPa. The selection range of the cyclic stress ratio ζ referred to the range of actual loads reported in previous studies [30], and followed the rule that the cyclic stress ratio decreases as the foundation depth deepens. Table 2 summarizes the drained cyclic triaxial test scheme of this study.

Table 2. Summary of the dynamic test programs.

Initial Mean Effective Stress, p_0(kPa)	Confining Pressure, σ_3(kPa)	Initial Static Stress Ratio, η_c	Cyclic Stress Ratio, ζ
40	26.7	1.0	1.0, 1.4, 1.8, 2.2
70	46.7	1.0	1.0, 1.4, 1.8, 2.2
100	66.8	1.0	0.2, 0.4, 0.6, 1.0, 1.8
200	133.3	1.0	0.2, 0.4, 0.6, 1.0, 1.8
300	150.0	1.0	0.2, 0.4, 0.6, 1.0, 1.8
400	266.7	1.0	0.4, 0.6, 1.0, 1.8

The strain of sample under cyclic loading includes resilient strain (${\varepsilon_1}^{ampl}$) and accumulated axial strain (${\varepsilon_1}^{acc}$). The typical hysteresis loop of the sample under cyclic loading is shown in Figure 4. The area of each hysteresis loop represents the energy dissipation per cycle, which characterizes the plastic work in a cycle, reflecting the resistance to deformation in profile. Resilient modulus (M_r) is an important parameter for the infrastructure of offshore islands and reefs, which is computed (Figure 4) by:

$$M_r = q^{ampl} / \varepsilon_1^{ampl} \tag{1}$$

where q^{ampl} is the amplitude of cyclic deviatoric stress. The definition of cyclic stress ratio ζ is the ratio of cyclic deviatoric stress to initial mean effective stress. The definition of initial static stress ratio η_c is the ratio of initial static deviatoric stress to initial mean effective stress.

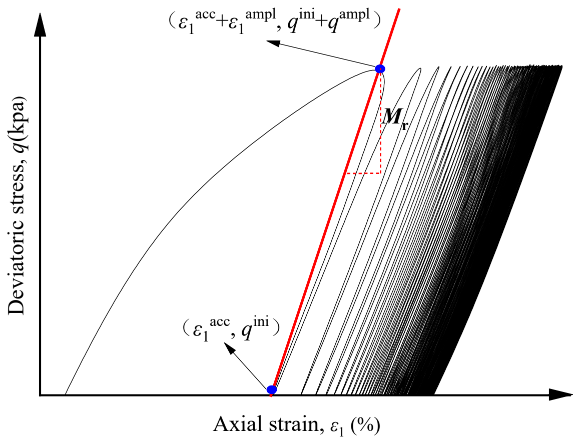

Figure 4. Typical hysteresis loop of the sample.

3. Results

3.1. Particle Breakage under Cyclic Loading

According to the fractal theory and Hardin's definition of relative particle breakage [31], Einav [32] proposed the relative particle breakage index to characterize the degree of particle breakage of coarse-grained soil. In the process of shearing, the gradation of coral sand changes to ultimate fractal gradation under high pressure. The ultimate gradation (as the basic property of the material) is independent of relative density and confining pressure, indicating that the particles will hardly break in the ultimate state. From this point of view, the index proposed by Einav [32] was used as a measure of particle breakage for coral sand:

$$B_r = \frac{B_t}{B_p} \tag{2}$$

where B_r is relative breakage index; B_p is total breakage potential; B_t is current total breakage potential. The ultimate gradation was obtained from the triaxial compression test under the maximum mean effective stress of 3 MPa (as shown in Figure 5). The total breakage potential B_p (as shown in Figure 5) can be acquired by integrating the area over the logarithmic scale:

$$B_p = \int_{d_m}^{d_M} [F_u(d) - F_0(d)] d(\log d) \tag{3}$$

where d_m is minimum diameter and d_M is maximum diameter. The total breakage B_t (as shown in Figure 5) can be calculated as:

$$B_t = \int_{d_m}^{d_M} [F_c(d) - F_0(d)] d(\log d) \tag{4}$$

The formulations $F_0(d)$, $F_c(d)$, and $F_u(d)$ (representing the initial gradation (IG), the current gradation (CG) and the ultimate gradation (UG) for coral sand, respectively, as shown in Figure 5) can be calculated as:

$$F_0(d) = (\frac{d}{d_M})^{3-\alpha_0} \tag{5}$$

$$F_c(d) = (\frac{d}{d_M})^{3-\alpha_c} \tag{6}$$

$$F_u(d) = (\frac{d}{d_M})^{3-\alpha_u} \tag{7}$$

where α_0, α_c, and α_u are fractal dimensions of IG, CG, and UG, respectively; d is diameter.

Substitution of Equations (3)–(7) into Equation (2) gives:

$$B_r = \frac{\int_{dm}^{d_M} [F_u(d) - F_0(d)] d(\log d)}{\int_{dm}^{d_M} [F_c(d) - F_0(d)] d(\log d)} = \frac{(\alpha_c - \alpha_0)(3 - \alpha_u)}{(\alpha_u - \alpha_0)(3 - \alpha_c)} \tag{8}$$

The initial fractal dimension and ultimate fractal dimension are supposed to 1.44 and 2.46, respectively, which were obtained by fitting the IG and UG (as shown in Figure 5).

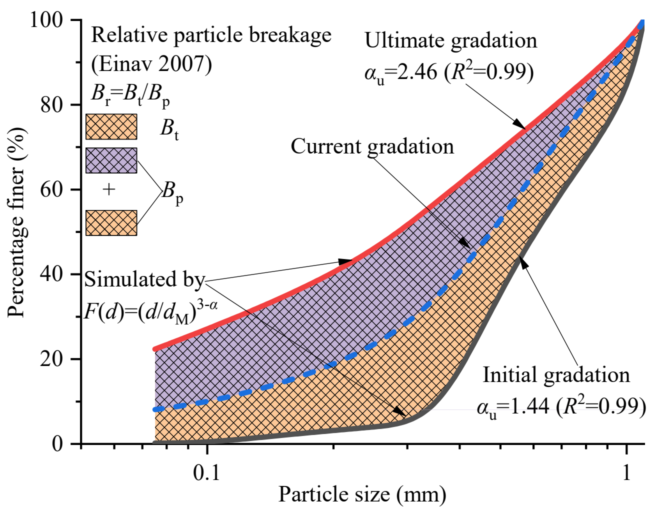

Figure 5. Definition of relative particle breakage index.

The fractal dimension α_c can be obtained by fitting current gradation using Equation (6). Figure 6 shows the fractal dimension α_c of coral sand at various initial mean effective stresses p_0. The larger the fractal dimension is, the more serious the particle breakage of coral sand is, and the more the particle gradation tends to the final fractal gradation. Under each p_0, in the range of lower cyclic stress ratio ζ, the α_c increases significantly with the increase of ζ; in the range of higher ζ, the rate of α_c increasing with ζ slows down. Under each ζ, the α_c of coral sand presents a consistent trend with the increase of the initial mean effective stress p_0. The α_c of coral sand shows a tendency of almost maintaining stable and then increasing rapidly with the increase of mean effective stress p_0. There is a threshold of p_0 (about 100 kPa), when the p_0 exceeds this threshold, α_c will increase significantly with the increase of p_0. This indicates that p_0 has a restrictive effect on the particle breakage of coral sand. When p_0 is small, the α_c (i.e., particle breakage) cannot grow fast. In actual engineering, it should be noted that when p_0 is greater than the threshold value, the significant and rapid increase of particle breakage will bring adverse effects on the service safety of the project. As can be seen in Figure 6, under each ζ, the α_c can be expressed as a function with p_0 as a variable:

$$\alpha_c = \alpha_{p0} + k_\alpha {\beta_\alpha}^{\log \frac{p_0}{p_a}} \tag{9}$$

where α_{p0}, k_α, and β_α are material parameters. The physical meaning of α_{p0} represents the fractal dimension of the starting particle breakage that can occur when the p_0 is relatively small at each ζ. The optimal regression value of k_α and β_α are 0.00575 and 147.955, respectively. The optimal regression values of α_{p0} at ζ = 0.2, 0.4, 0.6, 1.0, 1.4, 1.8, and 2.2 are 1.452, 1.522, 1.577, 1.619, 1.634, 1.648, and 1.661, respectively.

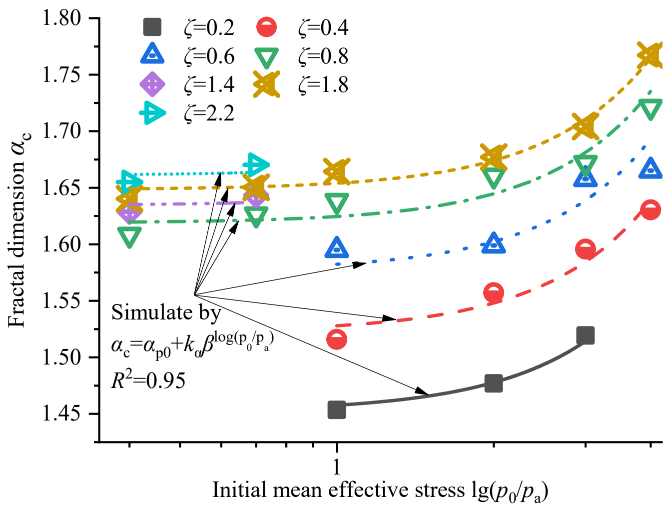

Figure 6. Fractal dimension of coral sand at various initial mean effective stresses.

Figure 7 shows the relationship between parameter α_{p0} and cyclic stress ratio ζ. The relationship between α_{p0} and ζ can be expressed as:

$$\alpha_{p0} = \chi_\alpha \zeta^{\mu_\alpha} \tag{10}$$

where χ_α and μ_α are material parameters. The optimal regression value of χ_α and $\zeta^{\mu\alpha}$ are 1.603 and 0.0550, respectively. Substitution of Equation (10) into Equation (9) gives:

$$\alpha_c = \alpha_{p0} + k_\alpha {\beta_\alpha}^{\log \frac{p_0}{p_a}} \tag{11}$$

Substitution of Equation (11) into Equation (8) gives:

$$B_r = \frac{(\chi_\alpha \zeta^{\mu_\alpha} + k_\alpha {\beta_\alpha}^{\log \frac{p_0}{p_a}} - \alpha_0)(3 - \alpha_u)}{(\alpha_u - \alpha_0)(3 - \chi_\alpha \zeta^{\mu_\alpha} - k_\alpha {\beta_\alpha}^{\log \frac{p_0}{p_a}})} \tag{12}$$

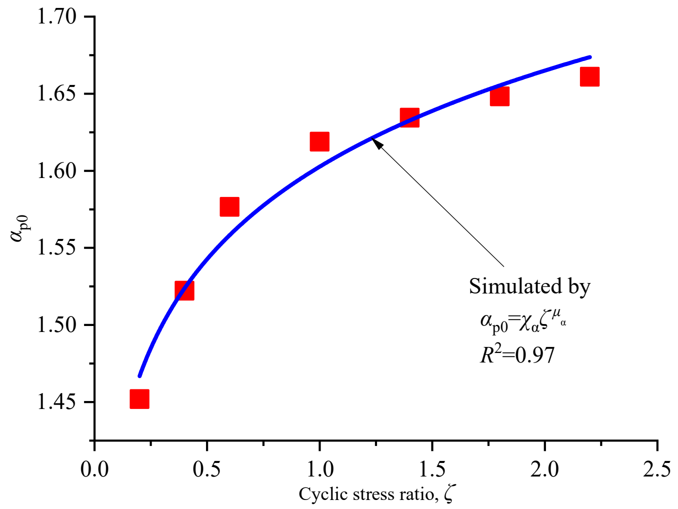

Figure 7. Relationship between parameter α_{p0} and cyclic stress ratio ζ.

At the end of the drained cyclic triaxial test, the calcareous sand sample was recovered carefully and the particle size distribution curve of the sample after cyclic loading was measured by the sieving test. Based on the observed particle size distribution curve after loading, the observed B_r of calcareous sand was then calculated by Equation (2). Figure 8 represents the relationship between B_r predicted by Equation (12) and observed B_r. It can be seen from Figure 8 that the points of predicted B_r and observed B_r are basically in a straight line with the slope of 1, indicating that Equation (12) can well predict the B_r of coral sand under cyclic loading. Substitution of Equation (10) into Equation (8) gives:

$$B_{rp0} = \frac{(\chi_\alpha \zeta^{\mu_\alpha} - \alpha_0)(3 - \alpha_u)}{(\alpha_u - \alpha_0)(3 - \chi_\alpha \zeta^{\mu_\alpha})} \tag{13}$$

where B_{rp0} is the starting relative particle breakage index that can occur when p_0 is relatively small at each ζ, which represents the ability of coral sand to resist particle breakage under different ζ.

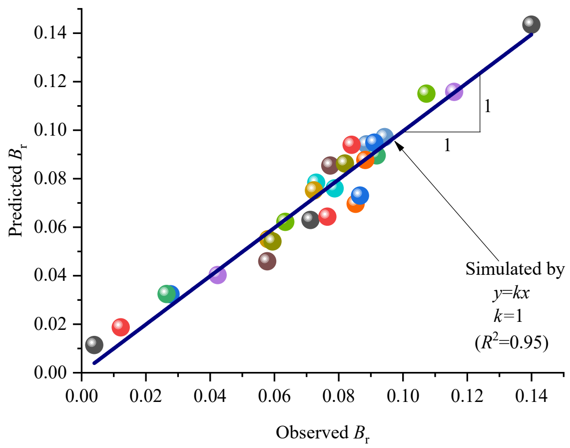

Figure 8. Comparison between observes B_r and predicted B_r.

3.2. Resilient Behavior under Cyclic Loading

Sun et al. [11] and Indraratna et al. [15] emphasized that understanding the resilient behavior of soil can be helpful to judge and avoid some factors that cause engineering accidents. Resilient modulus is an important design parameter for the safety evaluation of the infrastructures of ocean engineering. Therefore, a comprehensive understanding of the resilient modulus of coral sand is of great practical significance to the construction of reef island traffic infrastructures and the utilization of energy.

Figure 9 reflects the general evolution trend of the hysteresis loop of coral sand during cyclic loading. The cyclic stress ratio has a significant effect on the dynamic stress-strain relationship of calcareous sand. According to the changing trend of the shape and area of the hysteresis loop with the number of cycles N, the development law of the hysteresis loop under different cyclic stress ratios can be divided into two types. When the cyclic stress ratio ζ is small (ζ = 0.2), the hysteresis loop is closed at the beginning, and the area of hysteresis loop increases slightly with the increase of the number of cycles N. At the initial stage of cyclic loading, when the ζ is large (ζ = 0.4, 0.6 and 1.0), the opening of hysteresis loop is large and its shape is relatively irregular. With the development of cyclic loading, the opening of hysteretic loop tends to close, which is a long ellipse with two pointed ends. As the number of cycles increases, the dynamic strain accumulates, and the hysteresis loop becomes narrow. The area of the hysteresis loop decreases first and then increases slightly with the increase of N. Under the process of cyclic loading, the shape of coral sand's hysteresis loop changes rapidly at first, and then tends to be stable gradually. Roughly, in the early stage of cyclic loading, the hysteresis loop of coral sand first rotates anticlockwise, then slightly rotates clockwise in the later stage and finally tends to be stable. This illustrates that the resilient modulus M_r of coral sand under cyclic loading first increases with the number of cycles N, and then due to the continuous accumulation of particle breakage, the M_r will decrease to some extent in the later stage as N increases. Under the long-term cyclic loading, the M_r will finally tends to a stable value, which is consistent with the results of Sun et al. [11].

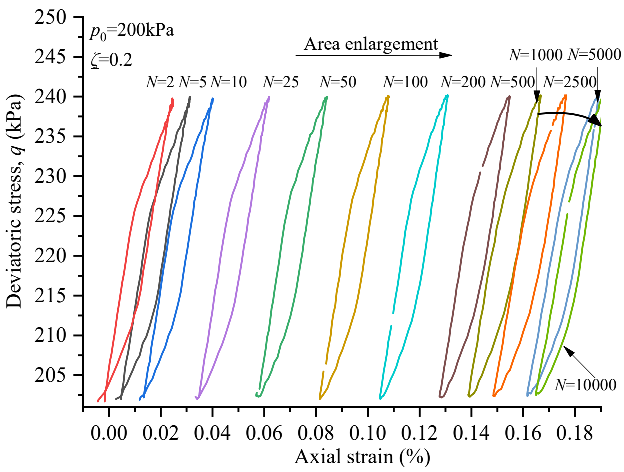

(a)

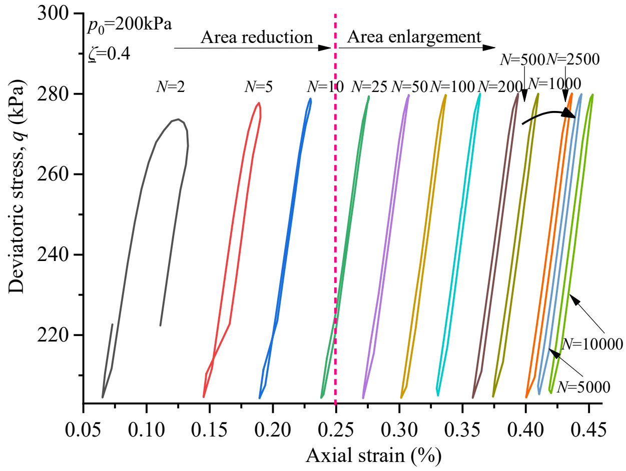

(b)

Figure 9. *Cont.*

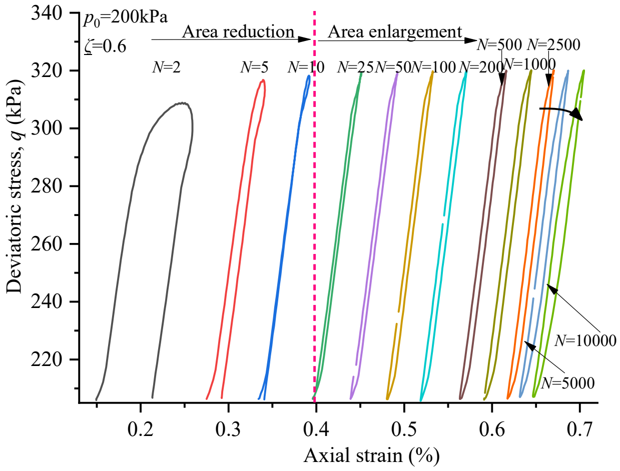

(c)

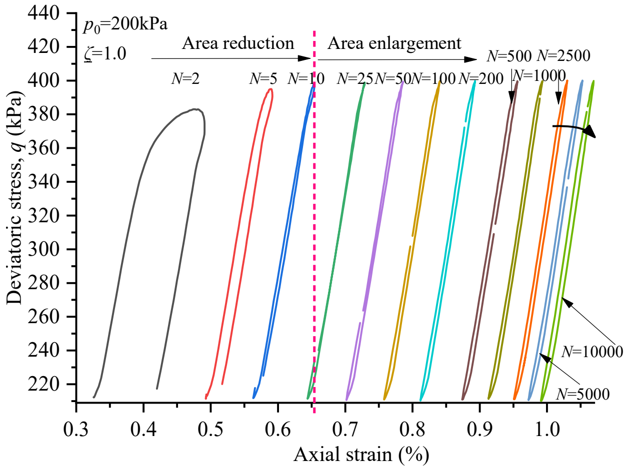

(d)

Figure 9. Hysteresis loop of coral sand under cyclic loading (take the samples of p_0 = 200k Pa as an example): (**a**) p_0 = 200 kPa, ζ = 0.2; (**b**) p_0 = 200 kPa, ζ = 0.4; (**c**) p_0 = 200 kPa, ζ = 0.6; (**d**) p_0 = 200 kPa, ζ = 1.0.

Figure 10a shows the variation of stable resilient modulus M_r^s with p_0. With the increase of p_0, M_r^s basically increases uniformly. This indicates that the increase of p_0 is beneficial for the improvement of M_r^s. This conclusion is consistent with the findings of Sun et al. [11] and Lackenby et al. [14]. Figure 10b shows the variation of stable resilient modulus with ζ. Contrary to the conclusion that M_r increases uniformly with the increase of ζ obtained by the experimental results on terrigenous granular materials [14], the M_r^s of coral sand only shows a slight growth trend as a whole. That is to say, as the ζ increases, the M_r^s does not increase uniformly but fluctuates. This indicates that the increase of ζ has both beneficial and detrimental effects on the improvement of the M_r^s. This phenomenon may be caused by the complexity and variability due to the particle breakage of coral sand material. It can be seen from Figure 6 that the particle breakage degree of coral sand increases with the increase of ζ and the particle breakage has an adverse effect on the stiffness; therefore, the cyclic stress ratio has a complex effect on the resilient modulus response of coral sand. This should be paid attention to in practical engineering.

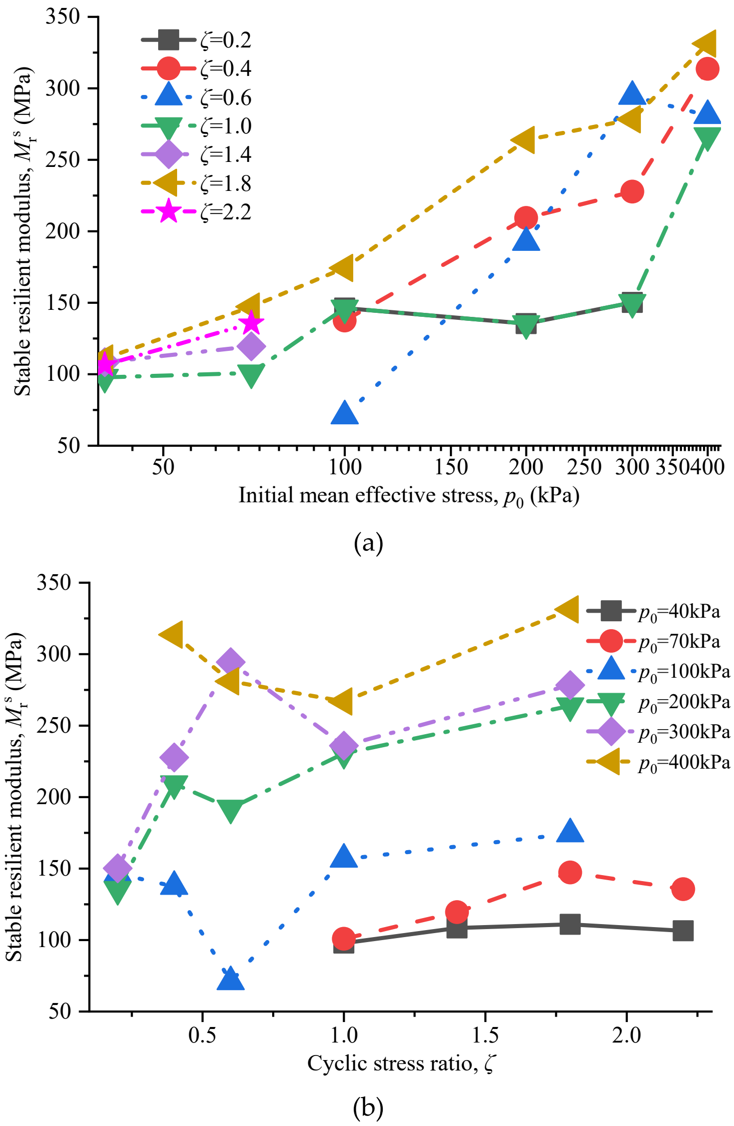

Figure 10. Stable resilient modulus of coral sand at various initial mean effective stress and cyclic stress ratios: (**a**) stable resilient modulus of coral sand at various initial mean effective stresses; (**b**) stable resilient modulus of coral sand at various cyclic stress ratios.

4. Discussion

The reasonable prediction of $M_r{}^s$ is of great significance to the actual engineering design and safety evaluation [10,33,34]. Therefore, Witczak and Uzan [35] established the empirical models for predicting the stable resilient modulus of terrigenous granular soil under cyclic loading. A famous two-parameter model proposed by Witczak and Uzan [33] only considered the cyclic deviatoric stress, not the initial mean effective stress p_0. Therefore, by introducing the initial mean effective stress into the model, the predicted resilient modulus $M_r{}^{ps}$ can be calculated as:

$$M_r{}^{ps} = k_1 \frac{p_0}{p_a} \zeta^{k_2} \tag{14}$$

where p_a = 100 kPa (i.e., standard atmospheric pressure); k_1 and k_2 are material parameters. The optimal regression value of k_1, k_2, k_3, and k_4 are 40.766, −0.297, −1553.306, and 0.282, respectively.

Figure 11 shows a comparison of the predicted surface of $M_r{}^{ps}$ calculated from Equation (14) with the observed $M_r{}^s$. As can be seen from Figure 11, the predicted $M_r{}^{ps}$ deviates greatly from the observed $M_r{}^s$. In the low stress range, the predicted $M_r{}^{ps}$ is always greater than the observed $M_r{}^s$, which has also been reported by many scholars when they study the granular soil with easily broken particles [21,36]. It can also be seen from Figure 11 that in the high stress range, the predicted $M_r{}^{ps}$ is always less than the observed $M_r{}^s$. The previous model for conventional terrestrial granular material cannot predict the $M_r{}^s$ of coral sand with easily broken particles in whole stress interval. Figure 12 shows the relationship between the ratio of predicted resilient modulus $M_r{}^{ps}$ by Equation (14) and observed $M_r{}^s$ with the particle breakage level $B_r p_0/p_a$. It can be obtained from Figure 12 that the particle breakage has a significant effect on the resilient modulus prediction model of coral sand. The $M_r{}^{ps}/M_r{}^s$ decreases with the increase of the $B_r p_0/p_a$, which indicates that the deviation between the predicted resilient modulus and the observed resilient modulus is partly caused by the difference of particle breakage level in various stress range. Coral sand has smaller particle breakage in the low stress range and larger particle breakage in the high stress range. The difference between particle breakage in the high and low stress ranges causes the predicted resilient modulus to regularly deviate from the observed resilient modulus. The starting relative particle breakage index B_{rp0} was introduced into the formula, and the prediction model of $M_r{}^{ps}$ considering the effect of particle breakage can be expressed as:

$$M_r{}^{ps} = k_1 \frac{p_0}{p_a} \zeta^{k_2} - k_3 B_{rp0} \left(\frac{p_0}{p_a}\right)^{k_4} \quad (15)$$

where p_a = 100 kPa (i.e., standard atmospheric pressure); B_{rp0} can be calculated by Equation (13); k_1, k_2, k_3, and k_4 are material parameters. The optimal regression value of k_1, k_2, k_3, and k_4 are 40.766, −0.297, −1553.306, and 0.282, respectively.

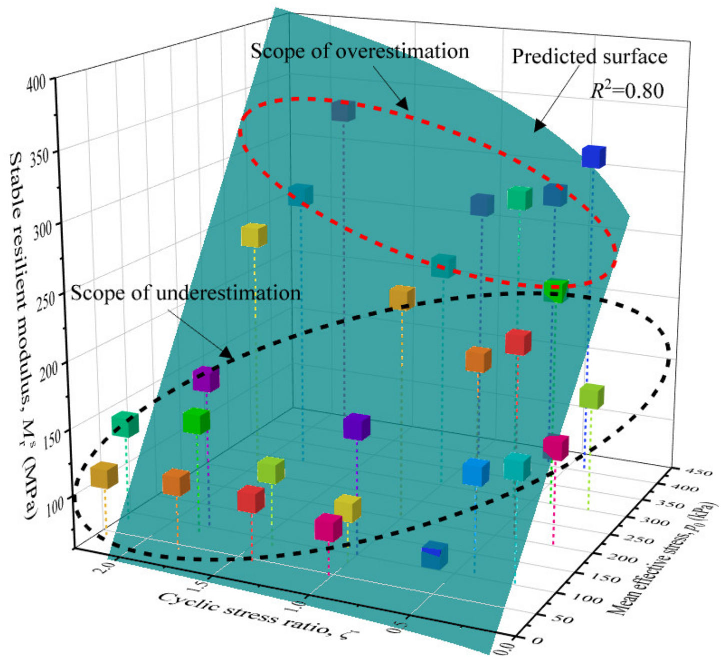

Figure 11. Predicted surface of stable resilient modulus calculated from Equation (14).

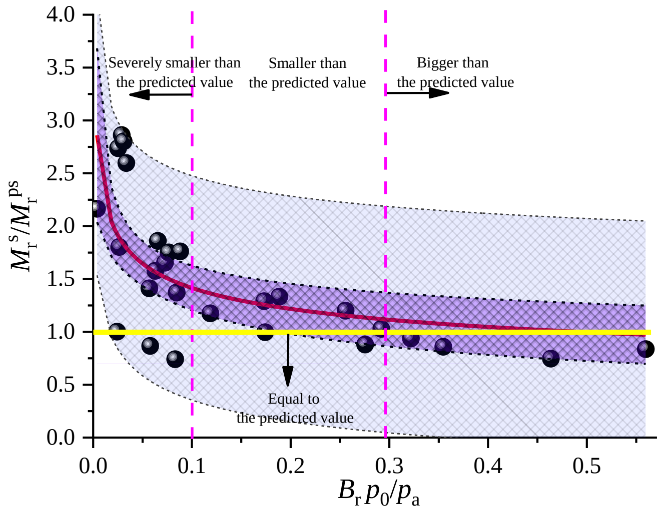

Figure 12. Relationship between $B_r p_0/p_a$ and M_r^{ps}/M_r^s calculated from Equation (14).

Figure 13 shows a comparison of the predicted surface of M_r^{ps} calculated from Equation (15) with the observed M_r^s. It can be seen from Figure 13 that the prediction model of the M_r^s considering particle breakage can make the predicted M_r^{ps} closer to the observed M_r^s. Figure 14 shows the relationship between the ratio of predicted resilient modulus M_r^{ps} by Equation (15) and observed M_r^s with the particle breakage level $B_r p_0/p_a$. It can be seen from Figure 14 that the M_r^{ps}/M_r^s is basically 1 and has no obvious relationship with the particle breakage level $B_r p_0/p_a$, which indicates that the prediction model of M_r^s considering particle breakage can better predict the resilient modulus response of coral sand. Therefore, unlike terrestrial granular materials, it is necessary to consider the impact of particle breakage when establishing a resilient modulus prediction model for coral sand. Considering particle breakage can help more accurately predict the resilient modulus of coral sand. In order to evaluate the resilient response of actual engineering more comprehensively and accurately, the effect of different particle sizes and relative densities on the prediction model of resilient modulus will be focused on in the future research. Moreover, the proposed formula will be verified in other types of soils.

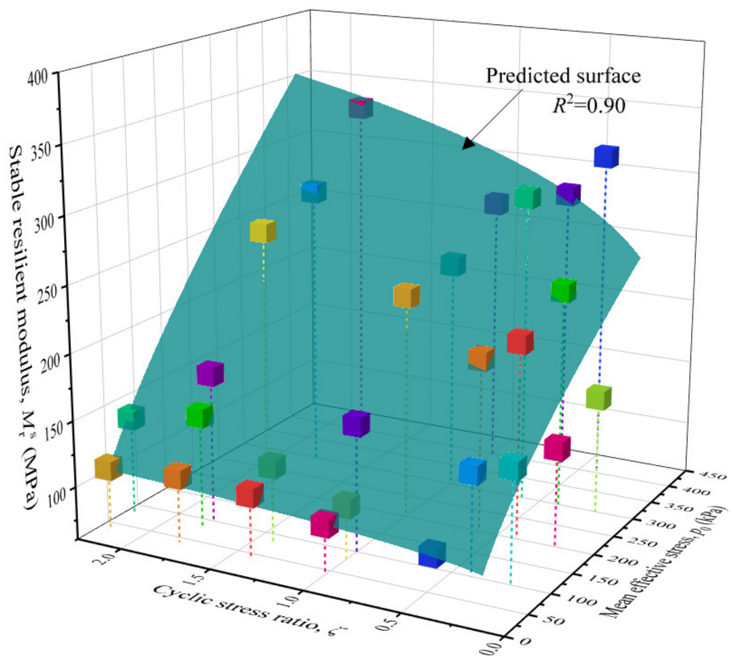

Figure 13. Predicted surface of stable resilient modulus calculated from Equation (15).

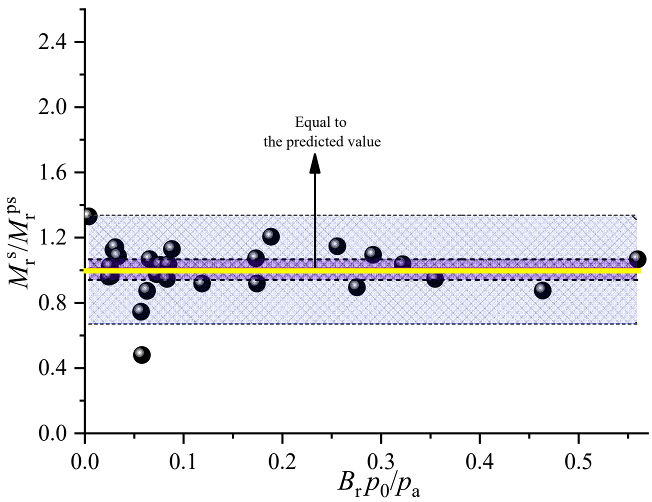

Figure 14. Relationship between $B_r p_0/p_a$ and M_r^{ps}/M_r^s calculated from Equation (15).

5. Conclusions

A series of drained cyclic triaxial tests were carried out on the coral sand of the South China Sea to investigate the resilient modulus M_r response and a new prediction model of M_r was proposed. The effects of the initial mean effective stress p_0 and cyclic stress ratio ζ on the M_r were examined. The main conclusions are the following:

(1) The change of fractal dimension α_c can reflect the rule of particle breakage evolution. The α_c of coral sand shows a tendency of almost maintaining stable and then increasing rapidly with the increase of mean effective stress p_0 under each cyclic stress ratio ζ. There is a threshold of p_0, when the p_0 exceed s this threshold, α_c will increase significantly with the increase of p_0. The actual project needs to pay attention to the adverse effect of the rapid increase of particle breakage on the engineering safety when p_0 is greater than the threshold.

(2) The resilient modulus M_r of coral sand under cyclic loading first increases with the number of cycles N, and then due to the continuous accumulation of particle breakage, the M_r will decrease to some extent in the later stage as N increases. Under the long-term cyclic loading, the M_r will finally tend to a stable value. The increase of p_0 has a beneficial effect on the improvement of the M_r, and the increase of p_0 will lead to the increase of M_r uniformly. The increase of ζ has both beneficial and detrimental effects on the improvement of the M_r, and the increase of ζ will cause the increase or decrease of M_r. The effect of ζ on the resilient modulus of coral sand is different from that of terrestrial granular materials, which is caused by the special material properties of coral sand.

(3) A new empirical prediction model of the M_r considering particle breakage was established, which can better predict the M_r of coral sand in the whole stress interval. Particle breakage has a significant effect on the prediction model of the M_r. It was found that if the particle breakage was not considered as an influencing factor in the empirical model, the predicted value of the M_r would deviate greatly from the measured value. Therefore, it is necessary to consider the effect of particle breakage when establishing a resilient modulus prediction model for the coral sand.

Author Contributions: Conceptualization, S.-H.H.; methodology, Z.D.; software, X.-L.G.; validation, T.-D.X. and Q.-F.Z.; formal analysis, S.-H.H.; investigation, Q.-F.Z.; resources, Z.D.; data curation, T.-D.X.; writing—original draft preparation, S.-H.H.; writing—review and editing, Z.D.; visualization, Q.-F.Z.; supervision, T.-D.X.; project administration, X.-L.G.; funding acquisition, Z.D. All authors have read and agreed to the published version of the manuscript.

Funding: This work was supported by the Chinese National Natural Science Foundation (Grant No. 51508506), Joint Fund of Zhejiang Provincial Natural Science Foundation (Grant No. LHZ20E080001) and Hangzhou

Science Technology Plan Project (Grant No. 20172016A06, 20180533B06, 20180533B12, 20191203B44); Advanced Postdoctoral Fund of Zhejiang Province (Grant No. 2019).

Acknowledgments: The authors are grateful for the comments of Bing-Qi Yu who have helped to significantly improve the article. Further, the authors appreciate the detailed checks and questions from the reviewers, which provide great help for the improvement of this article.

Conflicts of Interest: The authors declare no conflicts of interest.

References

1. Wang, X.; Jiao, Y.; Wang, R.; Hu, M.; Meng, Q.; Tian, F. Engineering characteristics of the calcareous sand in Nansha Islands, South China Sea. *Eng. Geol.* **2011**, *120*, 40–47. [CrossRef]
2. Shahnazari, H.; Rezvani, R. Effective parameters for the particle breakage of calcareous sands: An experimental study. *Eng. Geol.* **2013**, *159*, 98–105. [CrossRef]
3. Wang, X.Z.; Wang, X.; Jin, Z.; Zhu, C.; Wang, R.; Meng, Q. Investigation of engineering characteristics of calcareous soils from fringing reef. *Ocean Eng.* **2017**, *134*, 77–86. [CrossRef]
4. Jafarian, Y.; Javdanian, H.; Haddad, A. Strain-dependent dynamic properties of Bushehr siliceous-carbonate sand: Experimental and comparative study. *Soil Dyn. Earthq. Eng.* **2018**, *107*, 339–349. [CrossRef]
5. Yang, S.; Liu, W. Research on Unconstrained Compressive Strength and Microstructure of Calcareous Sand with Curing Agent. *J. Mar. Sci. Eng.* **2019**, *7*, 294. [CrossRef]
6. Wu, Q.; Ding, X.; Zhang, Y.; Chen, Z. Comparative Study on Seismic Response of Pile Group Foundation in Coral Sand and Fujian Sand. *J. Mar. Sci. Eng.* **2020**, *8*, 189. [CrossRef]
7. Shahnazari, H.; Rezvani, R.; Tutunchian, M.A. Post-cyclic volumetric strain of calcareous sand using hollow cylindrical torsional shear tests. *Soil Dyn. Earthq. Eng.* **2019**, *124*, 162–171. [CrossRef]
8. Patel, D.V.; Kumar, R.; Chauhan, K.A.; Patel, S. Experimental and Modeling Studies of Resilient Modulus and Permanent Strain of Stabilized Fly Ash. *J. Mater. Civil Eng.* **2019**, *31*, 06019005. [CrossRef]
9. Chen, W.; Jeng, D.; Chen, W.; Chen, G.; Zhao, H. Seismic-induced dynamic responses in a poro-elastic seabed: Solutions of different formulations. *Soil Dyn. Earthq. Eng.* **2020**, *131*, 106021. [CrossRef]
10. Han, Z.; Vanapalli, S.K. Relationship between resilient modulus and suction for compacted subgrade soils. *Eng. Geol.* **2016**, *211*, 85–97. [CrossRef]
11. Sun, Q.; Indraratna, B.; Nimbalkar, S. Deformation and degradation mechanisms of railway ballast under high frequency cyclic loading. *J. Geotech. Geoenviron.* **2016**, *142*, 04015056. [CrossRef]
12. Miao, Y.; Huang, Y.; Zhang, Q.; Wang, L. Effect of temperature on resilient modulus and shear strength of unbound granular materials containing fine RAP. *Constr. Build. Mater.* **2016**, *124*, 1132–1141. [CrossRef]
13. Hicks, R.G. Factors Influencing the Resilient Properties of Granular Materials. Ph.D. Thesis, Univ.of California, Berkeley, Berkeley, CA, USA, 1970.
14. Lackenby, J.; Indraratna, B.; McDowell, G.; Christie, D. Effect of confining pressure on ballast degradation and deformation under cyclic triaxial loading. *Geotechnique* **2007**, *57*, 527–536. [CrossRef]
15. Indraratna, B.; Biabani, M.M.; Nimbalkar, S. Behavior of geocell-reinforced subballast subjected to cyclic loading in plane-strain condition. *J. Geotech. Geoenviron.* **2015**, *141*, 04014081. [CrossRef]
16. Donohue, S.; Osullivan, C.; Long, M. Particle breakage during cyclic triaxial loading of a carbonate sand. *Geotechnique* **2009**, *59*, 477–482. [CrossRef]
17. Indraratna, B.; Lackenby, J.; Christie, D. Effect of confining pressure on the degradation of ballast under cyclic loading. *Geotechnique* **2005**, *55*, 325–328. [CrossRef]
18. Indraratna, B.; Tennakoon, N.; Nimbalkar, S.; Rujikiatkamjorn, C. Behavior of clay fouled ballast under drained triaxial testing. *Geotechnique* **2013**, *63*, 410–419. [CrossRef]
19. Cao, Z.; Chen, J.; Cai, Y.; Gu, C.; Wang, J. Effects of moisture content on the cyclic behavior of crushed tuff aggregates by large-scale tri-axial test. *Soil Dyn. Earthq. Eng.* **2017**, *95*, 1–8. [CrossRef]
20. Cao, Z.; Chen, J.; Cai, Y.; Zhao, L.; Gu, C.; Wang, J. Long-term behavior of clay-fouled unbound granular materials subjected to cyclic loadings with different frequencies. *Eng. Geol.* **2018**, *243*, 118–127. [CrossRef]
21. Chen, W.; Yin, J.; Feng, W.; Borana, L.; Chen, R. Accumulated permanent axial strain of a subgrade fill under cyclic high-speed railway loading. *Int. J. Geomech.* **2018**, *18*, 04018018. [CrossRef]
22. Uzan, J. Characterization of granular material. *Transp. Res. Rec.* **1985**, *1022*, 52–59.

23. Jafarian, Y.; Javdanian, H. Small-strain dynamic properties of siliceous-carbonate sand under stress anisotropy. *Soil Dyn. Earthq. Eng.* **2020**, *131*, 106045. [CrossRef]
24. Zheng, Q.; Xia, T.; Ding, Z.; He, S. The effect of periodic intermittency on the cyclic behavior of marine sedimentary clay. *Mar. Georesour. Geotechnol.* **2018**, *15*, 1–16. [CrossRef]
25. Cai, Y.; Hao, B.; Gu, C.; Wang, J.; Pan, L. Effect of anisotropic consolidation stress paths on the undrained shear behavior of reconstituted Wenzhou clay. *Eng. Geol.* **2018**, *242*, 23–33. [CrossRef]
26. Zhi, D.; Kong, B.; Wei, X.; Zhang, M.; Xu, B.; Zhao, F. Laboratory testing to research the micro-structure and dynamic characteristics of frozen-thawed marine soft soil. *J. Mater. Civil Eng.* **2019**, *7*, 85. [CrossRef]
27. Lin, B.; Zhang, F.; Feng, D.; Tang, K.; Feng, X. Accumulative plastic strain of thawed saturated clay under long-term cyclic loading. *Eng. Geol.* **2017**, *231*, 230–237. [CrossRef]
28. Wang, J.; Guo, L.; Cai, Y.; Xu, C.; Gu, C. Strain and pore pressure development on soft marine clay in triaxial tests with a large number of cycles. *Ocean Eng.* **2013**, *74*, 125–132. [CrossRef]
29. Ren, X.; Xu, Q.; Xu, C.; Teng, J.; Lv, S. Undrained pore pressure behavior of soft marine clay under long-term low cyclic loads. *Ocean Eng.* **2018**, *150*, 60–68. [CrossRef]
30. Guo, L.; Cai, Y.; Jardine, R.J.; Yang, Z.X.; Wang, J. Undrained behaviour of intact soft clay under cyclic paths that match vehicle loading conditions. *Can. Geotech. J.* **2018**, *55*, 90–106. [CrossRef]
31. Hardin, B.O. Crushing of Soil Particles. *J. Geotech. Geoenviron.* **1985**, *111*, 1177–1192. [CrossRef]
32. Einav, I. Breakage mechanics—Part I: Theory. *J. Mech. Phys. Solids.* **2007**, *55*, 1274–1297. [CrossRef]
33. Malla, R.B.; Joshi, S. Subgrade resilient modulus prediction models for coarse and fine-grained soils based on long-term pavement performance data. *Int. J. Pavement Eng.* **2008**, *9*, 431–444. [CrossRef]
34. Nazzal, M.D.; Mohammad, L.N. Estimation of Resilient Modulus of Subgrade Soils for Design of Pavement Structures. *J. Mater. Civil Eng.* **2010**, *22*, 726–734. [CrossRef]
35. Witczak, M.W.; Uzan, J. *The Universal Airport Pavement Design System: Report of IV: Granular Material Characterization*; College of Engineering, University of Maryland: College Park, MD, USA, 1988.
36. Yau, A.; Von Quintus, H. *Study of Laboratory Resilient Modulus Test Data and Response Characteristics. Final Rep. FHWA-RD-02-051*; Federal Highway Administration, U.S. Dept. of Transportation: Washington, DC, USA, 2002.